

1 Detecting turnover among complex communities using null models: A case study with sky-island  
2 haemosporidian parasites

3  
4 Lisa N. Barrow<sup>1,2</sup>, Selina M. Bauernfeind<sup>1</sup>, Paxton A. Cruz<sup>1</sup>, Jessie L. Williamson<sup>1</sup>, Daniele L.  
5 Wiley<sup>1</sup>, John E. Ford<sup>1</sup>, Matthew J. Baumann<sup>1</sup>, Serina S. Brady<sup>1</sup>, Andrea N. Chavez<sup>1,3,4</sup>, Chauncey  
6 R. Gadek<sup>1</sup>, Spencer C. Galen<sup>5</sup>, Andrew B. Johnson<sup>1</sup>, Xena M. Mapel<sup>1</sup>, Rosario A. Marroquin-  
7 Flores<sup>1,6</sup>, Taylor E. Martinez<sup>1,7</sup>, Jenna M. McCullough<sup>1</sup>, Jade E. McLaughlin<sup>1</sup>, Christopher C.  
8 Witt<sup>1\*</sup>

9  
10 <sup>1</sup>Museum of Southwestern Biology and Department of Biology, University of New Mexico,  
11 Albuquerque, NM

12 <sup>2</sup>Department of Evolution, Ecology and Organismal Biology, The Ohio State University,  
13 Columbus, OH

14 <sup>3</sup>Bureau of Land Management, Rio Puerco District Office, Albuquerque, NM

15 <sup>4</sup>Cibola National Forest and National Grasslands, Albuquerque, NM

16 <sup>5</sup>Department of Ornithology, Academy of Natural Sciences of Drexel University and Department  
17 of Biodiversity, Earth, and Environmental Sciences, Drexel University, Philadelphia, PA

18 <sup>6</sup>School of Biological Sciences, Illinois State University, Normal, IL

19 <sup>7</sup>Department of Molecular Medicine and Pharmacology, University of South Florida, Tampa, FL

20

21 \*Corresponding author: [cwitt@unm.edu](mailto:cwitt@unm.edu); 505-918-7199 (<https://orcid.org/0000-0003-2781-1543>)

22

23 **Abstract**

24 Turnover in species composition between sites, or beta diversity, is a critical component of  
25 species diversity that is typically influenced by geography, environment, and biotic interactions.  
26 Quantifying turnover is particularly challenging, however, in multi-host, multi-parasite  
27 assemblages where undersampling is unavoidable, resulting in inflated estimates of turnover and  
28 uncertainty about its spatial scale. We developed and implemented a framework using null  
29 models to test for community turnover in avian haemosporidian communities of three sky islands  
30 in the southwestern United States. We screened 776 birds for haemosporidian parasites from  
31 three genera (*Parahaemoproteus*, *Plasmodium*, and *Leucocytozoon*) by amplifying and  
32 sequencing a mitochondrial DNA barcode. We detected infections in 280 birds (36.1%),  
33 sequenced 357 infections, and found a total of 99 parasite haplotypes. When compared to  
34 communities simulated from a regional pool, we observed more unique, single-mountain  
35 haplotypes and fewer haplotypes shared among three mountain ranges than expected, indicating  
36 that haemosporidian communities differ to some degree among adjacent mountain ranges. These  
37 results were robust even after pruning datasets to include only identical sets of host species, and  
38 they were consistent for two of the three haemosporidian genera. The two more distant mountain  
39 ranges were more similar to each other than the one located centrally, suggesting that the  
40 differences we detected were due to stochastic colonization-extirpation dynamics. These results  
41 demonstrate that avian haemosporidian communities of temperate-zone forests differ on  
42 relatively fine spatial scales associated with adjacent sky-islands. Null models are essential tools  
43 for detecting turnover in complex, undersampled, and poorly known systems.

44

45 **Keywords:** Avian malaria, beta diversity, *Parahaemoproteus*, *Plasmodium*, *Leucocytozoon*

## 46 **Introduction**

47           The mechanisms that cause community composition to change across space are critical to  
48 the origin and maintenance of species diversity, and are therefore worthy of detailed study  
49 (Buckley and Jetz 2008; Socolar et al. 2016). Species diversity is traditionally partitioned into  
50 local (alpha) and regional (gamma) scales, with beta diversity, defined as species turnover  
51 between local communities, representing a link between local and regional processes (Whittaker  
52 1960, 1972). Beta diversity is affected by geographic distance, environmental factors (abiotic),  
53 and species interactions (biotic), and considerable efforts have been made to disentangle the roles  
54 of these various factors in determining community composition and structure (e.g., Fitzpatrick et  
55 al. 2013, Warburton et al. 2016, Clark et al. 2018). A major challenge for quantifying turnover,  
56 however, is the inability to fully sample the communities being compared. Sampling artifacts can  
57 either inflate or diminish beta diversity estimates because of undersampling, differences in  
58 abundance or detectability of species, or the proportion of rare species in a given system  
59 (Colwell and Coddington 1994; Chao et al. 2005; Cardoso et al. 2009). The issues of  
60 undersampling or biased sampling are especially complex in multi-host, multi-parasite  
61 assemblages in which parasite communities are nested within host communities (Poulin 1997;  
62 Krasnov et al. 2011), hosts and parasites have reciprocal filtering effects (Poulin 1999; Brooks et  
63 al. 2006; Thornhill and Fincher 2013), and undersampling of rare or host-specific microbial  
64 parasites is unavoidable (Hughes et al. 2001; Zhou et al. 2013; Poulin 2014).

65           Several studies have called attention to sampling effects on beta diversity estimation and  
66 have taken various approaches to address this issue. One suggested approach was to develop new  
67 beta diversity metrics that adjust for unsampled species (Chao et al. 2005, 2006), although these  
68 metrics still appear to be sensitive to sampling under certain conditions (Beck et al. 2013). Other

69 studies have attempted to identify beta diversity metrics that are less sensitive to sampling  
70 effects, in order to provide recommendations for which metrics are most appropriate to use for a  
71 given question and system (Cardoso et al. 2009; Beck et al. 2013). For example, the  $\beta_{-2}$   
72 (Harrison et al. 1992) and  $\beta_{-3}$  (Williams 1996) metrics were found to be particularly robust to  
73 undersampling but were insensitive to species richness differences between communities, such  
74 that other metrics may be preferred if richness differences are important (Cardoso et al. 2009).  
75 Rarefaction techniques, which adjust for sampling effort through random subsampling, are well-  
76 established for alpha diversity and have more recently been extended to estimate beta diversity  
77 (Dornelas et al. 2014; Stier et al. 2016). These methods can account for uneven sampling among  
78 sites and thus produce comparable relative estimates of beta diversity, but at the inevitable  
79 potential cost of removing data and statistical power. By reducing sampling, these approaches  
80 can lead to the appearance of community differences, leaving uncertainty about whether there is  
81 turnover or not.

82 Null models have also been highlighted as a useful tool for studying beta diversity that  
83 could be used to address sampling issues (Anderson et al. 2011). For example, Roden et al.  
84 (2018) used null models to demonstrate conditions under which beta diversity can be accurately  
85 estimated by focusing only on abundant taxa. Their conclusions rest on the assumption that  
86 patterns evident in dominant taxa can be extrapolated to the whole community; however, this  
87 may not be a suitable assumption for diverse pathogen or parasite communities in which rarer  
88 taxa can have ecological significance due to varying degrees of host-specialization and  
89 phenomena such as periodic host-switching (Brooks and Hoberg 2007; Woolhouse and Gaunt  
90 2007; Ricklefs et al. 2014). Ideally, community differences in complex host-parasite assemblages  
91 should be tested with a method that accounts for undersampling of parasites, uneven and

92 incomplete sampling of hosts, and substantial variation in abundance and host specialization  
93 among parasite species.

94         Here, we implement a null modeling framework to test for and investigate community  
95 turnover in the multi-host, multi-parasite assemblage of haemosporidian parasites and their avian  
96 hosts in the sky islands of the southwestern United States. These sky islands are defined by high-  
97 elevation forested habitats that are geographically isolated by low-elevation, arid habitats.  
98 Similar to archipelago systems (Ricklefs and Bermingham 2008), sky islands provide  
99 opportunities to study the factors that influence community structure, biogeographic patterns,  
100 and evolutionary diversification (Knowles 2001; McCormack et al. 2008; Gupta et al. 2019;  
101 Williamson et al. 2019). Avian haemosporidians include the intracellular, protozoan parasites  
102 that cause avian malaria, a global disease system that has been associated with epidemics,  
103 population declines, and extinction of naïve hosts (Warner 1968; van Riper et al. 1986; Atkinson  
104 and LaPointe 2009). These remarkably complex assemblages are becoming model systems for  
105 studying ecology and evolution of host-parasite interactions. At least three genera of  
106 haemosporidians (*Plasmodium*, *Parahaemoproteus*, and *Leucocytozoon*) commonly infect  
107 diverse bird communities with varying degrees of host specificity (Hellgren et al. 2009; Loiseau  
108 et al. 2012), abundance (Fallon et al. 2005; Ricklefs et al. 2011), and potential impacts on  
109 survival and fitness (Marzal et al. 2008; Knowles et al. 2010; Asghar et al. 2015). The  
110 geographic scale and potential drivers of haemosporidian community turnover have been  
111 investigated in several continental and island systems (e.g., Scordato and Kardish 2014, Ellis et  
112 al. 2015, Clark and Clegg 2017), but few consistent patterns have emerged across regions, host  
113 species, or parasite genera, underscoring the complexity of these systems.

114           On a global scale, haemosporidian communities do not appear to follow common patterns  
115 of biodiversity such as latitudinal gradients (Clark 2018; Fecchio et al. 2020). On a regional  
116 scale, host community turnover has been one of the most consistent predictors of haemosporidian  
117 community turnover across systems including Melanesia (Olsson-Pons et al. 2015; Clark et al.  
118 2018), South America (Fecchio et al. 2017), eastern North America (Ellis et al. 2015), and the  
119 Southwestern U.S. (Williamson et al. 2019). In contrast, geographic distance has been implicated  
120 in parasite community dissimilarity in some regions (West Indies: Fallon et al. 2005; South  
121 America: Fecchio et al. 2017), but not others (Asia: Scordato and Kardish 2014; Southwestern  
122 U.S.: Williamson et al. 2019). Distance-decay patterns also vary among haemosporidian genera,  
123 with *Plasmodium* exhibiting more geographic structure than *Parahaemoproteus* in two island  
124 systems (Fallon et al. 2003; Ishtiaq et al. 2010), despite the common finding that *Plasmodium*  
125 lineages tend to be more generalized and can be globally distributed (Hellgren et al. 2015;  
126 Walther et al. 2016). Similarly, environmental characteristics such as elevation and climate  
127 influence the distribution of haemosporidian genera in different ways, a finding that may be  
128 related to variation in the distribution of genus-specific vectors (Valkiunas 2005; van Rooyen  
129 et al. 2013; Galen and Witt 2014; Harrigan et al. 2014). In sum, disentangling the drivers of  
130 haemosporidian distributions is an exciting and active area of research, but one that is  
131 complicated by the effects of chronic undersampling.

132           Although sampling issues are unavoidable in avian haemosporidian studies, the influence  
133 of undersampling on estimates of community turnover have not been explicitly addressed.  
134 Instead, authors have taken pragmatic approaches such as including only well-sampled species or  
135 lineages in their analyses (Ellis et al. 2015; Soares et al. 2017), combining sites into regional  
136 communities for analysis (Clark 2018), choosing beta diversity metrics that are thought to be less

137 sensitive to sampling issues (Svensson-Coelho and Ricklefs 2011), or using rarefaction methods  
138 to evenly sample communities before estimating beta diversity metrics (Fecchio et al. 2019;  
139 Williamson et al. 2019). These and other previous studies of turnover were focused on obtaining  
140 comparable relative measures of beta diversity to test for its causes, but they may have neglected  
141 to address a more fundamental question: Are the communities different at all? This question is  
142 important to address with rigor because undersampling of parasite species or uneven sampling of  
143 host species may cause absolute estimates of beta diversity to exceed their true values.

144         The primary goal of our study was to test for turnover among haemosporidian parasite  
145 communities of three sky islands in northern New Mexico that are separated by >25 km of  
146 unforested habitat and that have near-identical host communities. We compared patterns among  
147 the full haemosporidian community of each sky island and, separately, the subsets of the  
148 communities comprised of each of the three parasite genera. We estimated the probability that  
149 species composition between communities differed after accounting for variation in abundance  
150 among parasite species and variation in sampling effort among sky islands. We then conducted  
151 four follow-up analyses to better understand our results. First, we assessed sensitivity of results  
152 to the host species sampled by repeating tests with only host species that were sampled from all  
153 three mountain ranges. Second, we assessed differences in turnover between specialist and  
154 generalist parasite lineages. Third, we assessed turnover among sky-island parasite communities  
155 of resident host species and migrant host species, respectively. Finally, we assessed turnover  
156 among sky island parasite communities within focal host species. While our surveys revealed  
157 many parasite haplotypes that occurred on only one or two sky islands, our null model approach  
158 was designed to test whether those lineages merely appeared to be restricted due to  
159 undersampling alone.

160

## 161 **Materials and methods**

### 162 **Sampling and parasite identification**

163           We sampled the breeding bird communities from three mountain ranges in northern New  
164 Mexico (Zuni Mountains, Mt. Taylor, and Jemez Mountains), as described in Marroquin-Flores  
165 *et al.* (2017). We conducted fieldwork between June and July 2016 (n = 186 samples) and 2017  
166 (n = 590 samples) in the transition zone between piñon-juniper woodland and ponderosa pine  
167 forests (elevation ~2100–2500 meters; Fig. 1). Birds were collected by mist-net or shotgun,  
168 preserved on dry ice, and transported to the Museum of Southwestern Biology (MSB) at the  
169 University of New Mexico for specimen preparation. Thin blood smears were prepared at the  
170 time of collection. In 2016, tissues (heart, pectoral muscle, liver) were preserved during  
171 specimen preparation at the MSB, and in 2017, tissues and whole blood were flash frozen in  
172 liquid nitrogen while in the field. All tissues are cryopreserved in liquid nitrogen at the MSB  
173 Division of Genomic Resources. Complete details for each specimen are available in Table A1  
174 (Online Resource 1) and its embedded links to the Arctos database. All samples were collected in  
175 accordance with animal care protocols and appropriate state and federal scientific collecting  
176 permits.

177           We extracted genomic DNA from 776 bird specimens, primarily from pectoral muscle,  
178 using QIAGEN DNeasy Blood and Tissue kits following the manufacturer's protocols. To  
179 identify haemosporidians from three genera (*Parahaemoproteus*, *Plasmodium*, *Leucocytozoon*),  
180 we used three nested PCR protocols to amplify 478 base pairs of the parasite mitochondrial  
181 cytochrome *b* (cytb) gene (Hellgren *et al.* 2004; Waldenström *et al.* 2004). Reaction conditions  
182 and thermal profiles are described in Marroquin-Flores *et al.* (2017). We visualized reaction



183 products on agarose gels to identify positive samples. We purified amplified products using  
184 ExoSap-IT and sequenced them in both directions using BigDye v3.1 terminator cycle  
185 sequencing and an ABI 3130 sequencer. Sequences were edited and assembled using Geneious  
186 v8.0 (<https://www.geneious.com>). We compared each sequenced infection to the MalAvi  
187 database (Bensch et al. 2009) using BLAST to determine the parasite genus. Then we either  
188 assigned known haplotype names for 100% matches or characterized parasite haplotypes as  
189 novel. We assigned names to novel haplotypes following MalAvi naming conventions, using the  
190 first three letters of both the genus and species of the first host species from which the haplotype  
191 was sequenced, followed by a number to denote multiple haplotypes from that host species (e.g.,  
192 SPIPAS02 for the second haplotype sequenced in *Spizella passerina*). Parasite sequences are  
193 archived on MalAvi and GenBank (Accession numbers MF077648–MF077690; MK216024–  
194 MK216290).

195       Microscopic examination of thin blood smears was conducted for 64% of samples,  
196 including all samples with positive PCR infections and for a portion of uninfected samples (n =  
197 494 total screened). Blood smears were air dried in the field, fixed in absolute methanol or  
198 ethanol, and stained for 50 min with Giemsa solution (pH 7.0). We examined blood smears using  
199 light microscopy, first scanning 10,000 erythrocytes at 200–400× magnification to locate and  
200 count *Leucocytozoon* infections. We then scanned 10,000 erythrocytes at 1000× magnification  
201 with an oil immersion lens to locate and count *Parahaemoproteus* and *Plasmodium* infections  
202 and take digital photographs of representative haemosporidians to archive in the Arctos database.  
203 We estimated infection intensity, or parasitemia, as the proportion of infected red blood cells out  
204 of 10,000 screened.

205

## 206 **Phylogenetic analysis and host specificity**

207           We estimated phylogenetic relationships among unique haemosporidian haplotypes using  
208 BEAST 2.4.8 (Bouckaert et al. 2014). To select an appropriate model of nucleotide substitution,  
209 we used PartitionFinder2 (Lanfear et al. 2017) with a search of all BEAST models and AICc  
210 model selection. We conducted BEAST analyses using the GTR+I+G model with estimated base  
211 frequencies, a relaxed lognormal clock, and two independent MCMC runs of 100 million  
212 generations each, sampling every 10,000 generations. We checked for convergence using Tracer  
213 v. 1.6 (Rambaut et al. 2018), confirming that ESS values for likelihoods and the majority of  
214 parameters were >1000. We then combined runs with LogCombiner using 10% burn-in, at which  
215 point stationarity was reached, and resampled states every 20,000 generations. We generated the  
216 maximum clade credibility (MCC) tree in TreeAnnotator from 9,002 posterior trees. Trees were  
217 rooted with the *Leucocytozoon* clade based on recent phylogenetic hypotheses for avian  
218 haemosporidians (Borner et al. 2016; Galen et al. 2018).

219           We obtained a phylogenetic hypothesis for the avian host species in our study from  
220 BirdTree.org, choosing the ‘Hackett all species’ set of trees (Hackett et al. 2008; Jetz et al.  
221 2012). To calculate indices of host specificity, we used the ‘picante’ package in R (Kembel et al.  
222 2010; R Core Team 2016). We report both a simple host specificity index, i.e., the total number  
223 of host species utilized, and a more complex index that incorporates host phylogenetic  
224 relationships and parasite abundance among hosts. The latter index is the weighted mean  
225 pairwise distance (MPD) developed for community phylogenetics (Webb et al. 2002) and has  
226 been applied previously to avian haemosporidians (e.g., Fallon et al. 2005, Svensson-Coelho et  
227 al. 2013). In brief, MPD describes the evolutionary diversity of hosts utilized by each parasite.  
228 To account for differences in sampling across parasites, we also calculated the standardized

229 effect size of MPD ( $SES_{MPD}$ ) using the null modeling procedure in ‘picante’ with the  
230 independent swap algorithm (Gotelli 2000), 1000 iterations, and 999 randomly generated host-  
231 parasite matrices.

232 We interpreted parasite lineages with negative values of  $SES_{MPD}$  ( $mpd.obs.z$ ) and low p-  
233 values ( $mpd.obs.p < 0.05$ ) as host specialists, while parasites with the highest values of  $SES_{MPD}$   
234 were considered to be host generalists. MPD could not be calculated for parasites sampled from a  
235 single host species, but we determined the minimum sample size needed to reject the hypothesis  
236 that a parasite is a host generalist, following Svensson-Coelho et al. (2013). Briefly, we  
237 determined that the probability of detecting a generalist parasite four or more times from a single  
238 host, and only that host, is extremely unlikely ( $p=0.043$ ), as follows. The best-sampled lineage  
239 with the highest skew in frequency in different host species was COLBF21 (10 of 22 infections  
240 were detected from the host species *Vireo plumbeus*, or 0.455). The probability that four random  
241 samples of this generalist parasite would occur in this same host is  $0.455^4 = 0.043$ , thus if we  
242 detected a parasite four or more times from one host species, we classified it as a host specialist.

243

#### 244 **Parasite community turnover**

245 We investigated haemosporidian community turnover among mountain ranges using a  
246 null modeling approach. We compared our observed sky-island communities to simulated  
247 communities expected under a model of no turnover, in which parasite communities in each  
248 mountain range are randomly sampled from the same hypothetical regional pool, with parasite  
249 richness (total number of haplotypes) and abundance distributions (frequency of each haplotype)  
250 based on empirical values derived from the combined data. Using the same framework, we tested  
251 for community differences using: 1) the full host-parasite dataset, 2) each parasite genus

252 (*Parahaemoproteus*, *Plasmodium*, *Leucocytozoon*) separately, 3) pruned datasets for the full and  
253 genus-level data including the set of identical host species sampled from all three mountain  
254 ranges ( $n = 26$  host species), 4) parasites classified as either host specialists or host generalists, 5)  
255 parasites of either migratory or resident host species, and 6) separate datasets for individual host  
256 species that were well-sampled ( $n > 20$  individuals) and included at least three parasite  
257 haplotypes from each mountain range. The modeling procedure, described below, was written as  
258 a set of functions in R and is available as electronic supplementary material (Online Resource 3).

259 *Observed sky-island communities:* The input file consisted of a data frame with all  
260 sequenced infections as rows, including the locality (mountain range), parasite genus, and  
261 haplotype name for each infection. These data were converted into two matrices of observed  
262 haplotypes (rows) per mountain range (columns); the first with abundances, or the number of  
263 infections observed (as in Fig. 2, right-most columns), and the second converted to a binary  
264 matrix that represents presence (1) or absence (0) of each haplotype in each mountain.

265 *Hypothetical regional community:* We combined the three observed communities and  
266 extrapolated to the total expected haplotype diversity using EstimateS v. 9.1.0 (Colwell et al.  
267 2012; Colwell 2013), while assuming that all three mountain ranges are part of a uniform  
268 regional community. We created a hypothetical list of haplotypes in the regional community,  
269 using the extrapolated total haplotype diversity as a starting point for parasite richness, and with  
270 an abundance distribution matching that of the observed communities. For example, if the  
271 original community of 99 haplotypes included 33 haplotypes (one-third) with an abundance of  
272 one, i.e., each haplotype was sequenced only once, then the hypothetical regional community  
273 with extrapolated diversity would also include one-third haplotypes with an abundance of one.

274           *Simulated sky-island communities:* We generated haplotype lists for the three mountain  
275 ranges by stochastically sampling infections from the hypothetical regional community, with  
276 replacement, up to the number of observed infections in each mountain range. The probability of  
277 sampling each haplotype was weighted by its abundance. We maintained equal richness between  
278 simulated and observed sky-island communities by keeping the first 10,000 simulated haplotype  
279 lists (i.e. simulated communities) for which the combined number of haplotypes matched that of  
280 the observed communities (n=99) once the target number of infections for each of the three  
281 mountain ranges had been reached.

282           *Test for non-random distribution of haplotype range sizes in the observed data:* In order  
283 to describe the distribution of range sizes for the simulated communities, we summed the number  
284 of haplotypes occurring in a single mountain, shared between two mountains, or occurring in all  
285 three mountains, respectively. We compared these sums for the observed data to the distribution  
286 of sums from the simulations to test whether, for example, there was an excess of small-ranged  
287 (single mountain) haplotypes observed. We calculated p-values as the proportion of simulations  
288 in which the number of haplotypes with a given range size (i.e., one, two, or three mountains)  
289 was greater than or equal to, or less than or equal to, respectively, the observed number of  
290 haplotypes with that range size.

291           *Test for non-random dissimilarity among mountain ranges:* For each pair of mountains,  
292 we calculated the Jaccard dissimilarity index for each simulation and compared the distribution  
293 of simulated values to the observed Jaccard values. We used the `vegdist()` function in the R  
294 package “vegan” (Oksanen et al. 2018). Jaccard indices provide a measure of dissimilarity on a  
295 scale from 0 (communities identical) to 1 (communities dissimilar). We calculated p-values as

296 the proportion of simulations that were greater than or equal to, or less than or equal to,  
297 respectively, the observed Jaccard indices between mountain pairs.

298 As an additional validation exercise, we compared the abundance distribution of range-  
299 restricted haplotypes between simulated and observed communities. In the simulated  
300 communities, range-restricted (single mountain range) haplotypes should be dominated by rare  
301 haplotypes because all of the haplotypes are assumed to be distributed throughout the region, i.e.,  
302 they come from the same regional pool. In the observed communities, at least some range-  
303 restricted haplotypes should have higher abundances while being truly range restricted.  
304 Accordingly, we predict that a cumulative frequency distribution (CFD) of range-restricted  
305 haplotypes grouped by abundance (haplotype count) should be right-shifted for the observed  
306 community relative to the simulated ones.

307

## 308 **Results**

### 309 **Parasite abundance and diversity**

310 We detected a total of 280 infected birds out of the 776 that were screened (overall  
311 prevalence of 36.1%). We observed parasites broadly across the avian community: 18 of 22  
312 families and 43 of 61 species were infected with haemosporidians. Based on PCR and  
313 sequencing results, 155 birds (20.0%) were infected with *Parahaemoproteus*, 62 (8.0%) with  
314 *Plasmodium*, and 105 (13.5%) with *Leucocytozoon*. Ninety birds (11.6%) were co-infected with  
315 two or more parasite haplotypes. Microscopic examination confirmed positive infections for 168  
316 birds and identified 11 additional infected birds that were not PCR-positive. The highest  
317 infection intensity detected was in a sample of *Aphelocoma woodhousii*, which had parasitemia

318 values of 4.8% for *Leucocytozoon* (sequences matched COLBF21/GYMCYA01) and 2.3% of  
319 *Parahaemoproteus* (sequence matched SPIPAS01).

320 Abundances of the three parasite genera differed somewhat among the three mountain  
321 ranges (Fig. 1). The highest overall prevalence (proportion of infected individuals from the total  
322 screened) was detected in the Jemez Mountains (42.0%), and Mt. Taylor and the Zuni Mountains  
323 were similar in prevalence, 32.4% and 31.6%, respectively. *Parahaemoproteus* was the most  
324 abundant genus in each of the mountain ranges, followed closely by *Leucocytozoon* in Jemez.  
325 *Plasmodium* was more abundant in the Zuni Mountains compared to the other two mountain  
326 ranges, where it was the least abundant parasite genus. Host clades and species also varied in  
327 prevalence (Fig. 2), with the lowest prevalence in suboscine passerines (10.8%) and the highest  
328 in Corvides (74.4%). The species with the highest overall prevalence was *Vireo plumbeus*, with  
329 87.2% of individuals infected.

330 A total of 357 infections were sequenced and assigned to 99 total haplotypes, including  
331 54 *Parahaemoproteus*, 12 *Plasmodium*, and 33 *Leucocytozoon* haplotypes. When compared to  
332 the MalAvi database, 55 (more than half, or a total of 56%) of these haplotypes were newly  
333 described from New Mexico; 27 of these were described from the 2016 field season and were  
334 reported previously (Marroquin-Flores et al. 2017). In that study, the total expected parasite  
335 richness for these communities was estimated to be ~70 (95% CI: 43–98) haplotypes. When we  
336 consider only the same 49 host species that were sampled in 2016 and included in the previous  
337 haplotype diversity predictions, we detected 96 parasite haplotypes in the 2017 host samples.  
338 This empirical result falls at the upper end of this predicted richness. Of the three mountain  
339 ranges, Jemez had the highest parasite richness (61 haplotypes) despite having the fewest birds  
340 sampled. We detected 53 haplotypes in Mt. Taylor and 47 haplotypes in Zuni.

341

## 342 **Phylogenetic relationships and host specialization**

343       The three haemosporidian genera were monophyletic with high posterior support,  
344 although relationships within each genus were less certain (Fig. 2). *Parahaemoproteus* and  
345 *Leucocytozoon* were detected in all host taxonomic groups sampled; *Plasmodium* was detected in  
346 all groups except non-passerines. Host breadth ranged from one to 14 hosts utilized, and MPD  
347 ranged from 0.9 to 20.7 with an average MPD of 10.2. Haemosporidians determined to be  
348 specialists were distributed across the parasite phylogeny, but they were most common in the  
349 genus *Parahaemoproteus*. Based on the  $SES_{MPD}$  metric, we classified 16 haemosporidians as  
350 specialists: 11 *Parahaemoproteus*, one *Plasmodium*, and four *Leucocytozoon* (Table 1). To  
351 assess community turnover between specialist and generalist parasites, we assigned the 16 most  
352 generalized parasites by considering those with the highest  $SES_{MPD}$  values. These included four  
353 *Parahaemoproteus*, five *Plasmodium*, and seven *Leucocytozoon*.

354

## 355 **Parasite community turnover**

356       More than half of the parasite haplotypes were unique to a single mountain range. Of the  
357 99 haplotypes, 56 were detected in one mountain range, 24 were shared among two mountain  
358 ranges, and only 19 were shared among all three mountain ranges. Comparing the observed data  
359 to the communities simulated under a model of no turnover indicated that there were more  
360 unique, single-mountain haplotypes ( $p < 0.001$ ) and fewer haplotypes shared among all three  
361 mountains than expected by chance ( $p = 0.027$ ; Fig. 3a). Turnover values between Mt. Taylor  
362 and the other two mountain ranges were higher than expected (Jemez-Mt. Taylor:  $p = 0.005$ , Mt.  
363 Taylor-Zuni:  $p = 0.01$ ; Fig. 3b). The pruned dataset with identical host species indicated



364 somewhat lower rates of turnover, with more unique haplotypes than expected ( $p = 0.013$ ; Fig.  
365 3c), no difference between the number of haplotypes shared among all three mountains ( $p =$   
366  $0.084$ ), and higher than expected turnover between Mt. Taylor and Jemez ( $p = 0.019$ ; Fig. 3d).

367 Results for *Parahaemoproteus* and *Leucocytozoon* were similar to the overall dataset. We  
368 found more single-mountain haplotypes than expected (*Parahaemoproteus*:  $p = 0.007$ ,  
369 *Leucocytozoon*:  $p = 0.023$ ; Fig. 3e,i) and higher turnover indices than expected by chance  
370 between Mt. Taylor and Jemez (*Parahaemoproteus*:  $p = 0.037$ , *Leucocytozoon*:  $p = 0.019$ ; Fig.  
371 3f,j). For *Parahaemoproteus*, Mt. Taylor and Zuni were also more different than expected ( $p =$   
372  $0.011$ ). We found no significant differences between observed and expected communities of  
373 *Plasmodium* (Fig. 3g,h). The pruned genus-level datasets indicated an excess of one-mountain  
374 haplotypes for *Parahaemoproteus* ( $p = 0.032$ ) and higher turnover than expected between Mt.  
375 Taylor and Jemez ( $p = 0.039$ ; Online Resource 2; Fig. A1).

376 Parasites classified as specialists or generalists, when analyzed separately, showed no  
377 significant differences between the observed and simulated communities (Table 2). The parasite  
378 communities of both migrant and resident host species, analyzed separately, showed similar  
379 results as the overall community dataset. We found more single-mountain haplotypes than  
380 expected (migrant:  $p = 0.007$ , resident:  $p = 0.009$ ), higher turnover than expected between Mt.  
381 Taylor and Zuni for migrant hosts ( $p = 0.04$ ), and higher turnover than expected between Mt.  
382 Taylor and Jemez for resident hosts ( $p = 0.013$ ; Table 2). Most of the focal host species showed  
383 no significant differences between observed and simulated communities, save for one of the best  
384 sampled hosts, *Vireo plumbeus*, which harbored fewer haplotypes that were shared between two  
385 mountain ranges than expected ( $p = 0.023$ ; Online Resource 2; Fig. A2). The abundance  
386 distribution of range-restricted (single-mountain) haplotypes in the observed community

387 indicated that at least some of these haplotypes were truly range-restricted because, rather than  
388 simply having low regional abundance, they were found 2–5 times on a single mountain, a  
389 phenomenon that was rarely observed in the simulated data (Online Resource 2; Fig. A3).

390

## 391 **Discussion**

392 Here, we screened hundreds of birds for haemosporidian parasites across three mountain  
393 ranges in northern New Mexico. We demonstrated that avian haemosporidian communities in  
394 northern New Mexico sky islands are highly diverse and differ over relatively fine spatial scales,  
395 even when the same set of host species and habitats are sampled. By increasing the sampling  
396 from a previous survey of these three mountain ranges four-fold, we elaborated general patterns  
397 of parasite abundance, diversity, specialization, and variation in infection rate among host  
398 species in this system. Our null model tests revealed an excess of localized (single mountain)  
399 parasite haplotypes and a deficit of shared haplotypes relative to expectations under a  
400 homogeneous regional community. These null models demonstrated that apparent turnover  
401 between mountain ranges is real in some cases, and not merely an artifact of undersampling. In  
402 other cases, undersampling can clearly create the appearance of turnover when there is none, and  
403 it can also exaggerate the degree of turnover as indicated by common metrics.

404 Improved sampling in this system, from 186 birds in Marroquin-Flores et al. (2017) to  
405 776 birds screened in the present study, showed that while parasite abundance remained highly  
406 consistent, parasite diversity had been underestimated. Overall prevalence (proportion of infected  
407 birds out of total screened) was 36.6% in 2016 and 36.1% in the combined-year dataset.  
408 Prevalence estimates for parasite genera were also consistent: *Parahaemoproteus* was estimated  
409 at 20.9%, and now at 20%; *Plasmodium* remained 8%, and *Leucocytozoon* was estimated at

410 13.4%, and now at 13.5%. The number of co-infections detected increased slightly in the  
411 combined-year dataset, from 9.7% to 11.6% of birds screened. *Parahaemoproteus* was the most  
412 common genus in all three mountain ranges, and consistently had the highest richness (54  
413 haplotypes, 55% of total), while *Plasmodium* had the lowest (12 haplotypes, 12% of total). Total  
414 parasite richness increased from 43 haplotypes detected in 2016 to 99 haplotypes total, which  
415 was higher than extrapolated diversity estimates (~70 haplotypes, 95% CI: 43–98) from the  
416 previous survey of these three mountain ranges (Marroquin-Flores et al. 2017). When only the 49  
417 host species sampled in 2016 were considered, we found 96 haplotypes, indicating that the  
418 addition of new host species alone does not account for this higher than expected diversity.  
419 Instead, a likely explanation is that true turnover between sites (beta diversity) exists and is an  
420 unaccounted for source of variation affecting these estimates, each of which was derived from  
421 the combined communities of the three mountains. When we extrapolate diversity from the full  
422 dataset, we continue to predict that a high proportion (~50%) of diversity in this system has yet  
423 to be discovered (~151 haplotypes, 95% CI: 115–188). These results indicate that extrapolated  
424 measures of diversity are likely to be underestimates when structured communities are analyzed  
425 together, or when there are any unmodeled sources of variation such as heterogeneous habitats or  
426 host communities.

427       Our results refined several interesting patterns related to variation in host breadth among  
428 parasites. Previously, *Parahaemoproteus* and *Leucocytozoon* were detected from only three of  
429 six host clades (Marroquin-Flores et al. 2017); here we found infections in all host clades,  
430 although both genera were still most common in Corvides and Passerides 1b (Fig. 2). Each of the  
431 three genera of haemosporidian parasites contained haplotypes that we classified as specialists  
432 and generalists, respectively, although *Parahaemoproteus* included the most host specialist

433 lineages and *Plasmodium* included the fewest. In previous work, clades of haemosporidian  
434 haplotypes associated with vireos have been noted in the western U.S. (Walther et al. 2016;  
435 Marroquin-Flores et al. 2017) and the eastern U.S. (Ricklefs et al. 2005). One outstanding  
436 question relates to whether these putative ‘vireo specialist’ parasites can establish successfully in  
437 other host species. Here we found that three of the 12 ‘vireo’ haplotypes did occur in other host  
438 clades, at least occasionally (Fig. 2). Only one of these infections out of eight screened by  
439 microscopic examination was confirmed to contain gametocytes. In this case, the parasite was  
440 VIRPLU04 and the host was a warbler, *Setophaga nigrescens*. This indicates that at least one of  
441 these vireo associated parasites is able to establish and reproduce in a non-vireo host.

442         Increased sampling also clarified patterns of variation in prevalence among host species.  
443 Previously, no infections in non-passerines or certain passerine species, such as nuthatches, were  
444 found in this system. While non-passerines were still rarely infected, we detected infections in  
445 six of 51 birds screened (11.8%) and three of these were confirmed by microscopic examination.  
446 Nuthatches also had very low prevalence; we did detect infections in five of 80 birds (6.25%) by  
447 PCR, but found no gametocytes in thin blood smears, suggesting that these might represent  
448 abortive infections of atypical hosts (Olias et al. 2011; Moens et al. 2016). At the clade level,  
449 suboscines were the least infected, a pattern that has been demonstrated consistently and has  
450 been used to illustrate that susceptibility to haemosporidians is evolutionarily conserved  
451 (Ricklefs 1992; Barrow et al. 2019). Corvids was the most infected host clade, with 58 of 78  
452 birds (74%) infected and a total of 97 infections detected. Vireos were among the host species  
453 with the highest prevalence; 87% of *Vireo plumbeus* and 78% of *V. gilvus* individuals were  
454 infected. Although sampling was limited (n=6), 100% of Woodhouse’s Scrub-Jay (*Aphelocoma*  
455 *woodhouseii*) individuals were infected and five of six were co-infected with *Leucocytozoon* and

456 one of the other two genera. Similarly high prevalences have been observed in *V. gilvus* in  
457 California (Walther et al. 2016) and in European corvids including crows and magpies  
458 (Scaglione et al. 2016; Schmid et al. 2017).

459 Null models were useful for detecting community differences while overcoming  
460 sampling inadequacies that are inevitable in complex, host-parasite systems. We found more  
461 unique parasite haplotypes (occurring in a single mountain) and fewer haplotypes shared across  
462 all three mountains than expected under a model of no turnover. When we pruned the dataset to  
463 include only identical host species across mountain ranges, these patterns were somewhat  
464 weaker, statistically, but consistent. Host community turnover is expected to play a role in  
465 parasite community turnover (Clark et al. 2018; Williamson et al. 2019). By effectively  
466 controlling for the host community, we demonstrate that haemosporidian parasite communities  
467 even differ among sky islands when the same set of host species are included. When considering  
468 the three genera separately, we found that both *Parahaemoproteus* and *Leucocytozoon* had  
469 similar patterns with the overall community, with more unique, single-mountain haplotypes than  
470 expected. *Plasmodium* did not show significant turnover patterns and, although this genus is rare  
471 in this system, this negative result was consistent with the expectation that *Plasmodium*  
472 haplotypes tend to be generalized and broadly distributed (e.g., Hellgren et al. 2015). Parasite  
473 turnover on fine spatial scales, such as between adjacent sky islands, is important because it  
474 implies that a single host species will encounter distinct parasite assemblages and associated  
475 diversifying selective pressures across its range.

476 Our results were consistent with previous studies demonstrating that geographic distance  
477 was not a consistent predictor of haemosporidian parasite turnover (Ellis et al. 2015; Williamson  
478 et al. 2019). Interestingly, the centrally-located mountain range in this system, Mt. Taylor,

479 exhibited the highest degree of turnover with the other two mountain ranges. These sampled  
480 communities are separated by a straight-line geographic distance of only ~50–100 km.  
481 Community differences on this fine scale are not unprecedented; Williamson et al. (2019) found  
482 high turnover in the haemosporidians of Audubon’s Warblers (*Setophaga auduboni*) sampled  
483 from eight mountain ranges in the southwestern U.S., including the three in the present study.  
484 The haemosporidian communities sampled in the Jemez and Zuni Mountains, separated by a  
485 distance of ~160 km, did not differ more than expected, a result that would have been difficult to  
486 interpret from a traditional beta diversity metric (Jaccard dissimilarity index: 0.615). Null model  
487 tests thus provided additional insights into the patterns of turnover in this system. The lack of the  
488 distance-decay relationship typical of some parasite systems (Poulin 2003; Thielges et al. 2009)  
489 has several possible explanations. Subtle habitat differences leading to changes in the vector  
490 community, which remains to be sampled and characterized, could influence some of the  
491 differences in parasite communities. The entire avian community, including host species not  
492 sampled in this study, also differs slightly between mountain ranges and partly explains parasite  
493 community turnover (Williamson et al. 2019). We suggest it is most likely that the turnover  
494 patterns we observed represent stochastic colonization-extirpation dynamics on sky islands.

495         We further explored these results by testing whether haemosporidian communities from  
496 migrant or resident hosts differed in patterns of turnover. Both migrant and resident host species  
497 had similar patterns compared to the overall host community, with more unique haplotypes than  
498 expected by chance, and community differences between Mt. Taylor and the other two mountain  
499 ranges. Long-distance migrants are expected to connect avian haemosporidian communities in  
500 breeding and wintering grounds, and greater connectivity between parasite faunas has been  
501 documented in the Americas (eastern North America and West Indies/northern South America)

502 compared to the Euro-African migration system (Hellgren et al. 2007; Ricklefs et al. 2017). Our  
503 results suggest that on a regional scale, migration does not strongly affect spatial community  
504 structure of avian haemosporidians, at least at the spatial scale of adjacent sky islands.

505 Here, we established a framework to compare communities in which sampling is  
506 inevitably incomplete and subject to stochastic variation. While accounting for several common  
507 sampling issues — skewed parasite-haplotype abundance distributions, uneven sampling among  
508 sites, different sets of host species, and habitats — we confirmed that avian haemosporidian  
509 turnover occurs on fine spatial scales, dispersal barriers of tens of kilometers, across which host  
510 turnover is negligible. Importantly, we were able to build on the work of Marroquin-Flores et al.  
511 (2017) because all data are available via museum specimens and open-access databases (Arctos,  
512 GenBank, and MalAvi). Likewise, future studies can continue building on these datasets to  
513 compare avian haemosporidian assemblages across mountain ranges, elevational zones, host  
514 communities, and focal host species. The differences we have already detected among nearby  
515 sites with sampling from the same habitats, elevations, and host communities suggest that adding  
516 sites with further habitat, climate, and host variation will provide rich datasets for understanding  
517 the drivers of diversity in this complex system.

518

## 519 **Acknowledgements**

520 We thank Michael Andersen, Sara Brant, Mariel Campbell, Joseph Manthey, Moses Michelsohn,  
521 and George Rosenberg. This work was supported by the Bureau of Land Management Rio  
522 Puerco Field Office (via the Colorado Plateau Cooperative Ecosystems Studies Unit agreement)  
523 and NSF DEB-1146491. SMB, RMF, and TEM were supported by PREP/FlyBase Fellowships

524 (NIH 5R25HG007630) and LNB was supported by an NSF Postdoctoral Research Fellowship in  
525 Biology (NSF DBI-1611710).

526

## 527 **References**

528 Anderson MJ, Crist TO, Chase JM, et al (2011) Navigating the multiple meanings of beta  
529 diversity: A roadmap for the practicing ecologist. *Ecol Lett* 14:19–28.

530 <https://doi.org/10.1111/j.1461-0248.2010.01552.x>

531 Asghar M, Hasselquist D, Hansson B, et al (2015) Hidden costs of infection: Chronic malaria  
532 accelerates telomere degradation and senescence in wild birds. *Science* 347:436–438.

533 <https://doi.org/10.1126/science.1261121>

534 Atkinson CT, LaPointe DA (2009) Introduced avian diseases, climate change, and the future of  
535 Hawaiian honeycreepers. *J Avian Med Surg* 23:53–63. <https://doi.org/10.1647/2008-059.1>

536 Barrow LN, McNew SM, Mitchell N, et al (2019) Deeply conserved susceptibility in a multi-  
537 host, multi-parasite system. *Ecol Lett* 22:987–998. <https://doi.org/10.1111/ele.13263>

538 Beck J, Holloway JD, Schwanghart W (2013) Undersampling and the measurement of beta  
539 diversity. *Methods Ecol Evol* 4:370–382. <https://doi.org/10.1111/2041-210x.12023>

540 Bensch S, Hellgren O, Pérez-Tris J (2009) MalAvi: a public database of malaria parasites and  
541 related haemosporidians in avian hosts based on mitochondrial cytochrome b lineages. *Mol*  
542 *Ecol Resour* 9:1353–1358. <https://doi.org/10.1111/j.1755-0998.2009.02692.x>

543 Borner J, Pick C, Thiede J, et al (2016) Phylogeny of haemosporidian blood parasites revealed  
544 by a multi-gene approach. *Mol Phylogenet Evol* 94:221–231.

545 <https://doi.org/10.1016/j.ympev.2015.09.003>

546 Bouckaert R, Heled J, Kuhnert D, et al (2014) BEAST 2: A software platform for Bayesian



- 547 evolutionary analysis. *PLoS Comput Biol* 10:e1003537.
- 548 <https://doi.org/10.1371/journal.pcbi.1003537>
- 549 Brooks DR, Hoberg EP (2007) How will global climate change affect parasite-host assemblages?  
550 *Trends Parasitol* 23:571–574. <https://doi.org/10.1016/j.pt.2007.08.016>
- 551 Brooks DR, León-Règagnon V, McLennan DA, Zelmer D (2006) Ecological fitting as a  
552 determinant of the community structure of platyhelminth parasites of anurans. *Ecology*  
553 87:S76–S85
- 554 Buckley LB, Jetz W (2008) Linking global turnover of species and environments. *Proc Natl*  
555 *Acad Sci* 105:17836–17841. <https://doi.org/10.1073/pnas.0803524105>
- 556 Cardoso P, Borges PAV, Veech JA (2009) Testing the performance of beta diversity measures  
557 based on incidence data: The robustness to undersampling. *Divers Distrib* 15:1081–1090.  
558 <https://doi.org/10.1111/j.1472-4642.2009.00607.x>
- 559 Chao A, Chazdon RL, Colwell RK, Shen TJ (2005) A new statistical approach for assessing  
560 similarity of species composition with incidence and abundance data. *Ecol Lett* 8:148–159.  
561 <https://doi.org/10.1111/j.1461-0248.2004.00707.x>
- 562 Chao A, Chazdon RL, Colwell RK, Shen TJ (2006) Abundance-based similarity indices and their  
563 estimation when there are unseen species in samples. *Biometrics* 62:361–371.  
564 <https://doi.org/10.1111/j.1541-0420.2005.00489.x>
- 565 Clark NJ (2018) Phylogenetic uniqueness, not latitude, explains the diversity of avian blood  
566 parasite communities worldwide. *Glob Ecol Biogeogr* 27:744–755.  
567 <https://doi.org/10.1111/geb.12741>
- 568 Clark NJ, Clegg SM (2017) Integrating phylogenetic and ecological distances reveals new  
569 insights into parasite host specificity. *Mol Ecol* 26:3074–3086.

- 570 <https://doi.org/10.1111/mec.14101>
- 571 Clark NJ, Clegg SM, Sam K, et al (2018) Climate, host phylogeny and the connectivity of host  
572 communities govern regional parasite assembly. *Divers Distrib* 24:13–23.  
573 <https://doi.org/10.1111/ddi.12661>
- 574 Colwell RK (2013) EstimateS: Statistical estimation of species richness and shared species from  
575 samples. Version 9. <http://purl.oclc.org/estimates>
- 576 Colwell RK, Chao A, Gotelli NJ, et al (2012) Models and estimators linking individual-based  
577 and sample-based rarefaction, extrapolation and comparison of assemblages. *J Plant Ecol*  
578 5:3–21. <https://doi.org/10.1093/jpe/rtr044>
- 579 Colwell RK, Coddington JA (1994) Estimating terrestrial biodiversity through extrapolation.  
580 *Philos Trans R Soc B Biol Sci* 345:101–118
- 581 Dornelas M, Gotelli NJ, McGill B, et al (2014) Assemblage time series reveal biodiversity  
582 change but not systematic loss. *Science* 344:296–299.  
583 <https://doi.org/10.1126/science.1248484>
- 584 Ellis VA, Collins MD, Medeiros MCI, et al (2015) Local host specialization, host-switching, and  
585 dispersal shape the regional distributions of avian haemosporidian parasites. *Proc Natl Acad*  
586 *Sci* 112:11294–11299. <https://doi.org/10.1073/pnas.1515309112>
- 587 Fallon SM, Bermingham E, Ricklefs RE (2005) Host specialization and geographic localization  
588 of avian malaria parasites: A regional analysis in the Lesser Antilles. *Am Nat* 165:466–480.  
589 <https://doi.org/10.1086/428430>
- 590 Fallon SM, Bermingham E, Ricklefs RE (2003) Island and taxon effects in parasitism revisited:  
591 Avian malaria in the Lesser Antilles. *Evolution* 57:606–615.  
592 [https://doi.org/https://doi.org/10.1554/0014-3820\(2003\)057\[0606:IATEIP\]2.0.CO;2](https://doi.org/https://doi.org/10.1554/0014-3820(2003)057[0606:IATEIP]2.0.CO;2)

- 593 Fecchio A, Bell JA, Bosholn M, et al (2020) An inverse latitudinal gradient in infection  
594 probability and phylogenetic diversity for Leucocytozoon blood parasites in New World  
595 birds. *J Anim Ecol* 89:423–435. <https://doi.org/10.1111/1365-2656.13117>
- 596 Fecchio A, Bell JA, Pinheiro RBP, et al (2019) Avian host composition, local speciation, and  
597 dispersal drive the regional assembly of avian malaria parasites in South American birds.  
598 *Mol Ecol* 28:2681–2693. <https://doi.org/10.1111/mec.15094>
- 599 Fecchio A, Pinheiro R, Felix G, et al (2017) Host community similarity and geography shape the  
600 diversity and distribution of haemosporidian parasites in Amazonian birds. *Ecography*  
601 (Cop) 41:505–515. <https://doi.org/10.1111/ecog.03058>
- 602 Fitzpatrick MC, Sanders NJ, Normand S, et al (2013) Environmental and historical imprints on  
603 beta diversity: Insights from variation in rates of species turnover along gradients. *Proc R*  
604 *Soc B Biol Sci* 280:20131201. <https://doi.org/10.1098/rspb.2013.1201>
- 605 Galen SC, Borner J, Martinsen ES, et al (2018) The polyphyly of *Plasmodium*: comprehensive  
606 phylogenetic analyses of the malaria parasites (order Haemosporida) reveal widespread  
607 taxonomic conflict. *R Soc Open Sci* 5:171780. <https://doi.org/10.1098/rsos.171780>
- 608 Galen SC, Witt CC (2014) Diverse avian malaria and other haemosporidian parasites in Andean  
609 house wrens: Evidence for regional co-diversification by host-switching. *J Avian Biol*  
610 45:374–386. <https://doi.org/10.1111/jav.00375>
- 611 Gotelli NJ (2000) Null model analysis of species co-occurrence patterns. *Ecology* 81:2606–2621
- 612 Gupta P, Vishnudas CK, Ramakrishnan U, et al (2019) Geographical and host species barriers  
613 differentially affect generalist and specialist parasite community structure in a tropical sky-  
614 island archipelago. *Proc R Soc B Biol Sci* 286:20190439.  
615 <https://doi.org/10.1098/rspb.2019.0439>

- 616 Hackett SJ, Kimball RT, Reddy S, et al (2008) A phylogenomic study of birds reveals their  
617 evolutionary history. *Science* 320:1763–8. <https://doi.org/10.1126/science.1157704>
- 618 Harrigan RJ, Sedano R, Chasar AC, et al (2014) New host and lineage diversity of avian  
619 haemosporidia in the northern andes. *Evol Appl* 7:799–811.  
620 <https://doi.org/10.1111/eva.12176>
- 621 Harrison S, Ross SJ, Lawton JH (1992) Beta diversity on geographic gradients in Britain. *J Anim*  
622 *Ecol* 61:151–158
- 623 Hellgren O, Atkinson CT, Bensch S, et al (2015) Global phylogeography of the avian malaria  
624 pathogen *Plasmodium relictum* based on MSP1 allelic diversity. *Ecography (Cop)* 38:842–  
625 850. <https://doi.org/10.1111/ecog.01158>
- 626 Hellgren O, Pérez-Tris J, Bensch S (2009) A jack-of-all-trades and still a master of some:  
627 Prevalence and host range in avian malaria and related blood parasites. *Ecology* 90:2840–  
628 2849. <https://doi.org/10.1890/08-1059.1>
- 629 Hellgren O, Waldenström J, Bensch S (2004) A new PCR assay for simultaneous studies of  
630 *Leucocytozoon*, *Plasmodium*, and *Haemoproteus* from avian blood. *J Parasitol* 90:797–802.  
631 <https://doi.org/10.1645/GE-184R1>
- 632 Hellgren O, Waldenström J, Pérez-Tris J, et al (2007) Detecting shifts of transmission areas in  
633 avian blood parasites - A phylogenetic approach. *Mol Ecol* 16:1281–1290.  
634 <https://doi.org/10.1111/j.1365-294X.2007.03227.x>
- 635 Hughes JB, Hellmann JJ, Ricketts TH, Bohannan BJM (2001) Counting the uncountable:  
636 Statistical approaches to estimating microbial diversity. *Appl Environ Microbiol* 67:4399–  
637 4406. <https://doi.org/10.1128/AEM.67.10.4399>
- 638 Ishtiaq F, Clegg SM, Phillimore AB, et al (2010) Biogeographical patterns of blood parasite

- 639 lineage diversity in avian hosts from southern Melanesian islands. *J Biogeogr* 37:120–132.  
640 <https://doi.org/10.1111/j.1365-2699.2009.02189.x>
- 641 Jarvis A, Reuter HI, Nelson A, Guevara E (2008) Hole-filled seamless SRTM data V4. *Int Cent*  
642 *Trop Agric* available from <http://srtm.csi.cgiar.org>
- 643 Jetz W, Thomas GH, Joy JB, et al (2012) The global diversity of birds in space and time. *Nature*  
644 491:444–448. <https://doi.org/10.1038/nature11631>
- 645 Kembel SW, Cowan PD, Helmus MR, et al (2010) Picante: R tools for integrating phylogenies  
646 and ecology. *Bioinformatics* 26:1463–1464. <https://doi.org/10.1093/bioinformatics/btq166>
- 647 Knowles LL (2001) Did the Pleistocene glaciations promote divergence? Tests of explicit  
648 refugial models in montane grasshoppers. *Mol Ecol* 10:691–701.  
649 <https://doi.org/10.1046/j.1365-294X.2001.01206.x>
- 650 Knowles SCL, Palinauskas V, Sheldon BC (2010) Chronic malaria infections increase family  
651 inequalities and reduce parental fitness: experimental evidence from a wild bird population.  
652 *J Evol Biol* 23:557–569. <https://doi.org/10.1111/j.1420-9101.2009.01920.x>
- 653 Krasnov BR, Stanko M, Khokhlova IS, et al (2011) Nestedness and  $\beta$ -diversity in ectoparasite  
654 assemblages of small mammalian hosts: Effects of parasite affinity, host biology and scale.  
655 *Oikos* 120:630–639. <https://doi.org/10.1111/j.1600-0706.2010.19072.x>
- 656 Lanfear R, Frandsen PB, Wright AM, et al (2017) Partitionfinder 2: New methods for selecting  
657 partitioned models of evolution for molecular and morphological phylogenetic analyses.  
658 *Mol Biol Evol* 34:772–773. <https://doi.org/10.1093/molbev/msw260>
- 659 Loiseau C, Harrigan RJ, Robert A, et al (2012) Host and habitat specialization of avian malaria  
660 in Africa. *Mol Ecol* 21:431–441. <https://doi.org/10.1111/j.1365-294X.2011.05341.x>
- 661 Marroquin-Flores RA, Williamson JL, Chavez AN, et al (2017) Diversity, abundance, and host

- 662 relationships in the avian malaria community of New Mexico pine forests. *PeerJ* 5:e3700.  
663 <https://doi.org/10.7717/peerj.3700>
- 664 Marzal A, Bensch S, Reviriego M, et al (2008) Effects of malaria double infection in birds: One  
665 plus one is not two. *J Evol Biol* 21:979–987. <https://doi.org/10.1111/j.1420->  
666 [9101.2008.01545.x](https://doi.org/10.1111/j.1420-9101.2008.01545.x)
- 667 McCormack JE, Bowen BS, Smith TB (2008) Integrating paleoecology and genetics of bird  
668 populations in two sky island archipelagos. *BMC Biol* 6:1–12.  
669 <https://doi.org/10.1186/1741-7007-6-28>
- 670 Moens MAJ, Valkiūnas G, Paca A, et al (2016) Parasite specialization in a unique habitat:  
671 hummingbirds as reservoirs of generalist blood parasites of Andean birds. *J Anim Ecol*  
672 85:1234–1245. <https://doi.org/10.1111/1365-2656.12550>
- 673 Oksanen J, Blanchet FG, Friendly M, et al (2018) *vegan: Community Ecology Package*. Version  
674 2.5-2. <https://CRAN.R-project.org/package=vegan>.
- 675 Olias P, Wegelin M, Zenker W, et al (2011) Avian malaria deaths in parrots, Europe. *Emerg*  
676 *Infect Dis* 17:950–952. <https://doi.org/10.1086/605025>
- 677 Olsson-Pons S, Clark NJ, Ishtiaq F, Clegg SM (2015) Differences in host species relationships  
678 and biogeographic influences produce contrasting patterns of prevalence, community  
679 composition and genetic structure in two genera of avian malaria parasites in southern  
680 Melanesia. *J Anim Ecol* 84:985–998. <https://doi.org/10.1111/1365-2656.12354>
- 681 Poulin R (1997) Species richness of parasite assemblages: Evolution and patterns. *Annu Rev*  
682 *Ecol Syst* 28:341–358. <https://doi.org/10.1146/annurev.ecolsys.28.1.341>
- 683 Poulin R (1999) The functional importance of parasites in animal communities: many roles at  
684 many levels? *Int J Parasitol* 29:903–914

- 685 Poulin R (2014) Parasite biodiversity revisited: Frontiers and constraints. *Int J Parasitol* 44:581–  
686 589. <https://doi.org/10.1016/j.ijpara.2014.02.003>
- 687 Poulin R (2003) The decay of similarity with geographical distance in parasite communities of  
688 vertebrate hosts. *J Biogeogr* 30:1609–1615
- 689 R Core Team (2016) R: A language and environment for statistical computing. [https://www.R-](https://www.R-project.org/)  
690 [project.org/](https://www.R-project.org/)
- 691 Rambaut A, Drummond AJ, Xie D, et al (2018) Posterior summarization in Bayesian  
692 phylogenetics using Tracer 1.7. *Syst Biol* 67:901–904.  
693 <https://doi.org/10.1093/sysbio/syy032>
- 694 Ricklefs R, Bermingham E (2008) The West Indies as a laboratory of biogeography and  
695 evolution. *Philos Trans R Soc B Biol Sci* 363:2393–2413.  
696 <https://doi.org/10.1098/rstb.2007.2068>
- 697 Ricklefs RE (1992) Embryonic development period and the prevalence of avian blood parasites.  
698 *Proc Natl Acad Sci* 89:4722–4725. <https://doi.org/10.1073/pnas.89.10.4722>
- 699 Ricklefs RE, Dodge Gray J, Latta SC, Svensson-Coelho M (2011) Distribution anomalies in  
700 avian haemosporidian parasites in the southern Lesser Antilles. *J Avian Biol* 42:570–584.  
701 <https://doi.org/10.1111/j.1600-048X.2011.05404.x>
- 702 Ricklefs RE, Medeiros M, Ellis VA, et al (2017) Avian migration and the distribution of malaria  
703 parasites in New World passerine birds. *J Biogeogr* 44:1113–1123.  
704 <https://doi.org/10.1111/jbi.12928>
- 705 Ricklefs RE, Outlaw DC, Svensson-Coelho M, et al (2014) Species formation by host shifting in  
706 avian malaria parasites. *Proc Natl Acad Sci U S A* 111:14816–21.  
707 <https://doi.org/10.1073/pnas.1416356111>

- 708 Ricklefs RE, Swanson BL, Fallon SM, et al (2005) Community relationships of avian malaria  
709 parasites in southern Missouri. *Ecol Monogr* 75:543–559. <https://doi.org/10.1890/04-1820>
- 710 Roden VJ, Kocsis ÁT, Zuschin M, Kiessling W (2018) Reliable estimates of beta diversity with  
711 incomplete sampling. *Ecology* 99:1051–1062. <https://doi.org/10.1002/ecy.2201>
- 712 Scaglione FE, Cannizzo FT, Pregel P, et al (2016) Blood parasites in hooded crows (*Corvus*  
713 *corone cornix*) in Northwest Italy. *Vet Ital* 52:111–116.  
714 <https://doi.org/10.12834/VetIt.110.307.2>
- 715 Schmid S, Facht K, Dinkel A, et al (2017) Carrion crows (*Corvus corone*) of southwest  
716 Germany: Important hosts for haemosporidian parasites. *Malar J* 16:1–12.  
717 <https://doi.org/10.1186/s12936-017-2023-5>
- 718 Scordato ESC, Kardish MR (2014) Prevalence and beta diversity in avian malaria communities:  
719 Host species is a better predictor than geography. *J Anim Ecol* 83:1387–1397.  
720 <https://doi.org/10.1111/1365-2656.12246>
- 721 Soares L, Latta SC, Ricklefs RE (2017) Dynamics of avian haemosporidian assemblages through  
722 millennial time scales inferred from insular biotas of the West Indies. *Proc Natl Acad Sci*  
723 114:6635–6640. <https://doi.org/10.1073/pnas.1702512114>
- 724 Socolar JB, Gilroy JJ, Kunin WE, Edwards DP (2016) How should beta-diversity inform  
725 biodiversity conservation? *Trends Ecol Evol* 31:67–80.  
726 <https://doi.org/10.1016/j.tree.2015.11.005>
- 727 Stier AC, Bolker BM, Osenberg CW (2016) Using rarefaction to isolate the effects of patch size  
728 and sampling effort on beta diversity. *Ecosphere* 7:e01612.  
729 <https://doi.org/10.1002/ecs2.1612>
- 730 Svensson-Coelho M, Blake JG, Loiselle BA, et al (2013) Diversity, prevalence, and host



- 731 specificity of avian *Plasmodium* and *Haemoproteus* in a Western Amazon assemblage.  
732 Ornithol Monogr 76:1–47. <https://doi.org/10.1525/om.2013.76.1.1.1>
- 733 Svensson-Coelho M, Ricklefs RE (2011) Host phylogeography and beta diversity in avian  
734 haemosporidian (Plasmodiidae) assemblages of the Lesser Antilles. J Anim Ecol 80:938–  
735 946. <https://doi.org/10.1111/j.1365-2656.2011.01837.x>
- 736 Thieltges DW, Ferguson MAD, Jones CS, et al (2009) Distance decay of similarity among  
737 parasite communities of three marine invertebrate hosts. Oecologia 160:163–173.  
738 <https://doi.org/10.1007/s00442-009-1276-2>
- 739 Thornhill R, Fincher CL (2013) The parasite-driven-wedge model of parapatric speciation. J  
740 Zool 291:23–33. <https://doi.org/10.1111/jzo.12070>
- 741 Valkiunas G (2005) Avian malaria parasites and other haemosporidia. CRC Press, Boca Raton,  
742 Florida, USA
- 743 van Riper C, van Riper SG, Goff ML, Laird M (1986) The epizootiology and ecological  
744 significance of malaria in Hawaiian land birds. Ecol Monogr 56:327–344.  
745 <https://doi.org/10.2307/1942550>
- 746 van Rooyen J, Lalubin F, Glaizot O, Christe P (2013) Altitudinal variation in haemosporidian  
747 parasite distribution in great tit populations. Parasites and Vectors 6:1–10.  
748 <https://doi.org/10.1186/1756-3305-6-139>
- 749 Waldenström J, Bensch S, Hasselquist D, Östman Ö (2004) A new nested polymerase chain  
750 reaction method very efficient in detecting *Plasmodium* and *Haemoproteus* infections from  
751 avian blood. J Parasitol 90:191–194. <https://doi.org/10.1645/GE-3221RN>
- 752 Walther EL, Carlson JS, Cornel A, et al (2016) First molecular study of prevalence and diversity  
753 of avian haemosporidia in a central California songbird community. J Ornithol 157:549–

- 754 564. <https://doi.org/10.1007/s10336-015-1301-7>
- 755 Warburton EM, Kohler SL, Vonhof MJ (2016) Patterns of parasite community dissimilarity: The  
756 significant role of land use and lack of distance-decay in a bat-helminth system. *Oikos*  
757 125:374–385. <https://doi.org/10.1111/oik.02313>
- 758 Warner RE (1968) The role of introduced diseases in the extinction of the endemic Hawaiian  
759 avifauna. *Condor* 70:101–120. <https://doi.org/10.2307/1365954>
- 760 Webb CO, Ackerly DD, McPeck MA, Donoghue MJ (2002) Phylogenies and community  
761 ecology. *Annu Rev Ecol Syst* 33:475–505.  
762 <https://doi.org/10.1146/annurev.ecolsys.33.010802.150448>
- 763 Whittaker RH (1960) Vegetation of the Siskiyou Mountains, Oregon and California. *Ecol*  
764 *Monogr* 30:279–338. <https://doi.org/10.2307/1943563>
- 765 Whittaker RH (1972) Evolution and the measurement of species diversity. *Taxon* 21:213–251
- 766 Williams PH (1996) Mapping variations in the strength and breadth of biogeographic transition  
767 zones using species turnover. *Proc R Soc B Biol Sci* 263:579–588.  
768 <https://doi.org/10.1098/rspb.1996.0087>
- 769 Williamson JL, Wolf CJ, Barrow LN, et al (2019) Ecology, not distance, explains community  
770 composition in parasites of sky-island Audubon’s Warblers. *Int J Parasitol* 49:437–448.  
771 <https://doi.org/10.1016/j.ijpara.2018.11.012>
- 772 Woolhouse M, Gaunt E (2007) Ecological origins of novel human pathogens. *Crit Rev Microbiol*  
773 33:231–242. <https://doi.org/10.1080/10408410701647560>
- 774 Zhou J, Jiang Y-H, Deng Y, et al (2013) Random sampling process leads to overestimation of  
775 Beta diversity of microbial communities. *MBio* 4:e00324-13.  
776 <https://doi.org/10.1128/mBio.00324-13.Editor>  
777

## 778 **Figure Captions**

779 Figure 1. Map of study areas and mountain ranges sampled. The number of individual birds  
780 sampled, host species sampled, birds infected, and infections detected using molecular methods  
781 are shown for each mountain. H = *Parahaemoproteus*, P = *Plasmodium*, L = *Leucocytozoon*.  
782 Elevation is based on the SRTM Digital Elevation Database (Jarvis et al. 2008).

783  
784 Figure 2. Phylogenetic relationships of haemosporidian haplotypes found in New Mexico birds.  
785 Columns represent host clades (left), host species (center), and mountain ranges (right). Dotted  
786 line indicates non-monophyly of non-passerines. Host species phylogeny was generated from  
787 <http://BirdTree.org> and branch colors correspond with host clades. Parasite phylogeny was  
788 estimated in BEAST and branches with posterior probabilities less than 0.7 were collapsed for  
789 visualization. Stars indicate novel haemosporidian haplotypes. “S” indicates haplotypes  
790 classified as specialists. Bar plots depict the combined infection rate (number of infections  
791 divided by number of birds screened). The number of infections sequenced for each haplotype in  
792 each host clade, host species, or mountain range is shown within matrix cells.

793  
794 Figure 3. Null model results for full dataset (a,b), pruned dataset with identical host species (c,d),  
795 and the three parasite genera (e-j). Distributions are density plots from 10,000 simulations and  
796 summarize the number of haplotypes found in one, two, or three mountains (a,c,e,g,i) or the  
797 Jaccard indices between each pair of mountains (b,d,f,h,j). Dotted lines indicate observed values  
798 for each test. \* indicates the observed value is significantly different ( $p < 0.05$ ) from the  
799 simulated communities, assessed as the proportion of simulated values that are greater than, less  
800 than, or equal to the observed value.

## Tables

Table 1. Host specificity indices for haemosporidian haplotypes sampled at least twice ( $n \geq 2$ ). MPD is the weighted mean pairwise distance calculated in the ‘picante’ R package. The standardized effect size of MPD ( $SES_{MPD}$ ) and P-values were estimated using 999 randomizations. \* indicates significantly specialized parasites ( $P < 0.05$  or sampled 4 or more times from a single host).

Haplotype	N	Host species	MPD	$SES_{MPD}$	P-value	Classified as:
H_PACPEC02	6	3	5.667	-2.266	0.019*	Specialist
H_PIRLUD02	8	1	NA	NA	*	Specialist
H_PIRFLA01	6	3	11.222	-0.547	0.259	
H_SETAUD14	2	2	13.000	0.911	0.813	Generalist
H_SPIPAS01	14	5	8.980	-2.689	0.011*	Specialist
H_SPIPAS02	8	3	8.000	-1.618	0.070	
H_CHOGRA01	5	1	NA	NA	*	Specialist
H_JUHYE03	2	2	6.000	-0.974	0.189	
H_PIRLUD01	6	1	NA	NA	NA*	Specialist
H_TROAED12	15	3	6.738	-1.859	0.060	
H_VIRPLU04	10	4	12.160	-0.923	0.177	
H_VIRPLU01	17	5	10.228	-2.185	0.033*	Specialist
H_VIGIL07	3	2	0.889	-2.543	0.013*	Specialist
H_SIAMEX01	4	1	NA	NA	*	Specialist
H_TABI02	2	2	2.000	-2.145	0.048*	Specialist
H_GYMCYA02	3	2	0.889	-2.348	0.012*	Specialist
H_SPISAL01	4	2	8.250	-0.418	0.297	Generalist
H_TACTHA02	5	1	NA	NA	*	Specialist
H_EMPOBE02	2	2	4.000	-1.621	0.099	
H_CYASTE05	4	2	9.750	-0.060	0.393	Generalist
H_PIRLUD07	3	2	13.333	0.974	0.879	Generalist
P_MOLATE01	6	5	16.778	0.235	0.554	Generalist
P_SEIAUR01	3	3	12.000	-0.348	0.314	Generalist
P_BAERID01	2	2	1.000	-2.457	0.025*	Specialist
P_TACTHA01	3	3	11.111	-0.662	0.237	
P_TACRUB04	2	2	14.000	1.215	0.939	Generalist
P_PADOM09	3	3	17.778	1.348	0.927	Generalist
P_TROAED24	18	8	17.148	-0.531	0.274	Generalist
P_LAIRI01	30	14	18.427	-1.286	0.098	
L_CB1	7	4	14.367	-0.226	0.359	Generalist
L_CYASTE07	4	1	NA	NA	*	Specialist
L_PIPMAC02	4	3	9.250	-1.265	0.116	
L_SETGRA02	9	2	6.222	-1.006	0.180	
L_PIRLUD03	5	2	0.960	-2.354	0.012*	Specialist
L_VIGIL08	3	3	16.889	1.044	0.862	Generalist
L_APHCAL01	6	4	14.222	-0.281	0.344	Generalist
L_COLBF21	22	11	19.289	-0.006	0.488	Generalist
L_SETNIG01	8	8	20.688	1.197	0.894	Generalist
L_GYMCYA01	6	4	15.667	0.155	0.511	Generalist
L_VIRPLU05	4	1	NA	NA	*	Specialist
L_CNEORN01	3	2	7.111	-0.863	0.181	
L_SETAUD25	2	2	8.000	-0.515	0.250	Generalist
L_PIRFLA02	5	3	6.880	-1.940	0.048*	Specialist

Table 2. Null model results for specialist or generalist parasites, and migrant or resident host species. The number of haplotypes observed in a single mountain or shared between two or three mountains, and the Jaccard indices between each pair of mountains are compared to the expected values from 10,000 simulated communities. P-values were calculated as the proportion of simulated values that are greater than, less than, or equal to the observed.

		Observed	Expected	P-value (Exp $\geq$ Obs)	P-value (Exp $\leq$ Obs)
<b>Specialist parasites</b>					
Number of haplotypes	1 mountain	1	1.814	0.896	0.407
	2 mountains	5	4.198	0.414	0.796
	3 mountains	6	5.988	0.642	0.652
Jaccard index	Jemez-Taylor	0.5	0.326	0.111	0.957
	Jemez-Zuni	0.167	0.356	0.968	0.058
	Taylor-Zuni	0.364	0.368	0.565	0.555
<b>Generalist parasites</b>					
Number of haplotypes	1 mountain	1	1.889	0.895	0.398
	2 mountains	7	5.036	0.188	0.927
	3 mountains	7	8.076	0.857	0.353
Jaccard index	Jemez-Taylor	0.333	0.355	0.647	0.465
	Jemez-Zuni	0.4	0.251	0.111	0.957
	Taylor-Zuni	0.357	0.357	0.546	0.568
<b>Migrant hosts</b>					
Number of haplotypes	1 mountain	46	37.019	0.007*	0.997
	2 mountains	21	26.375	0.926	0.117
	3 mountains	17	20.607	0.940	0.12
Jaccard index	Jemez-Taylor	0.653	0.582	0.065	0.94
	Jemez-Zuni	0.627	0.591	0.225	0.778
	Taylor-Zuni	0.672	0.594	0.043*	0.957
<b>Resident hosts</b>					
Number of haplotypes	1 mountain	21	15.613	0.009*	0.999
	2 mountains	5	9.461	0.982	0.05
	3 mountains	4	4.925	0.855	0.389
Jaccard index	Jemez-Taylor	0.852	0.699	0.013*	0.989
	Jemez-Zuni	0.609	0.625	0.584	0.418
	Taylor-Zuni	0.789	0.699	0.113	0.888

**Figure 1**

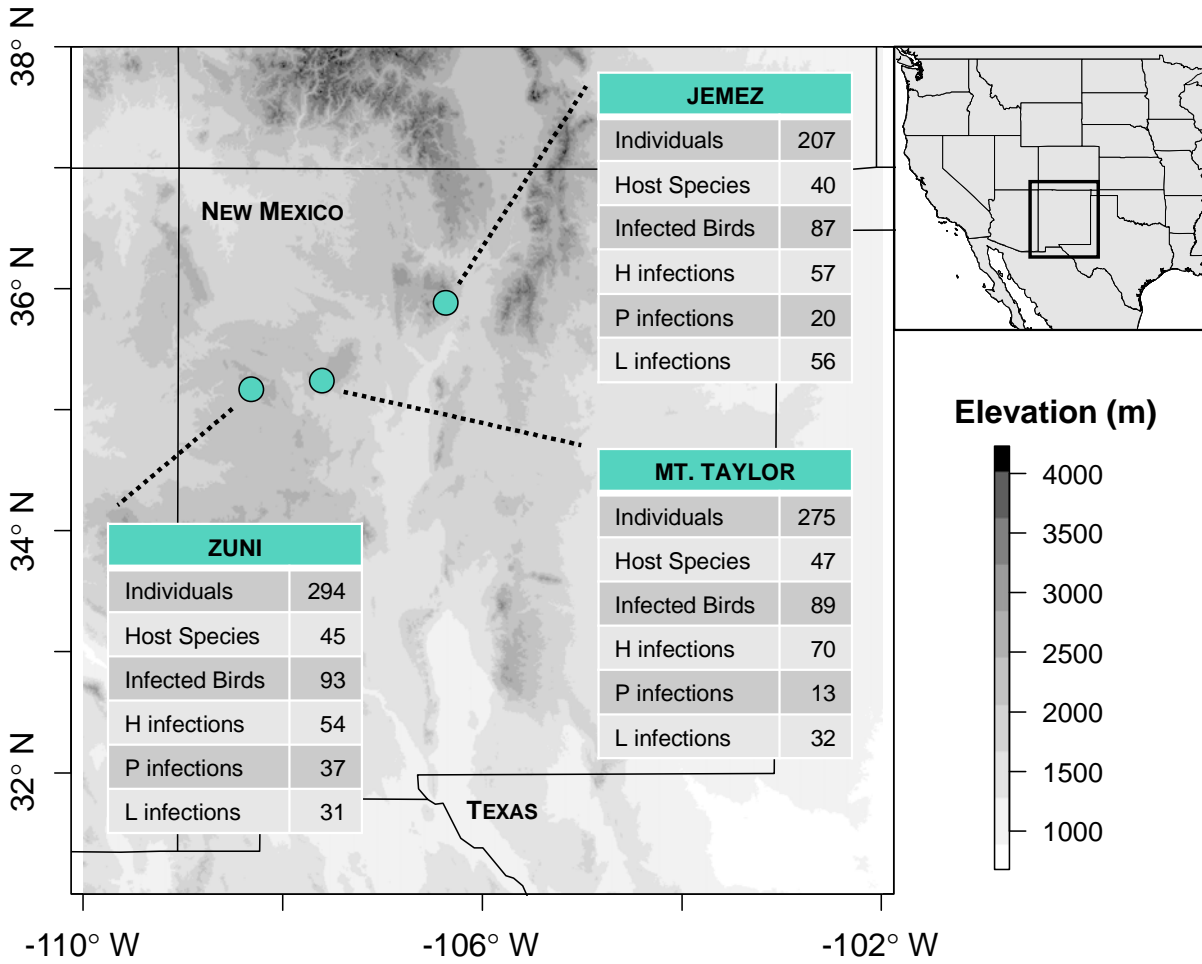




**Figure 3**

